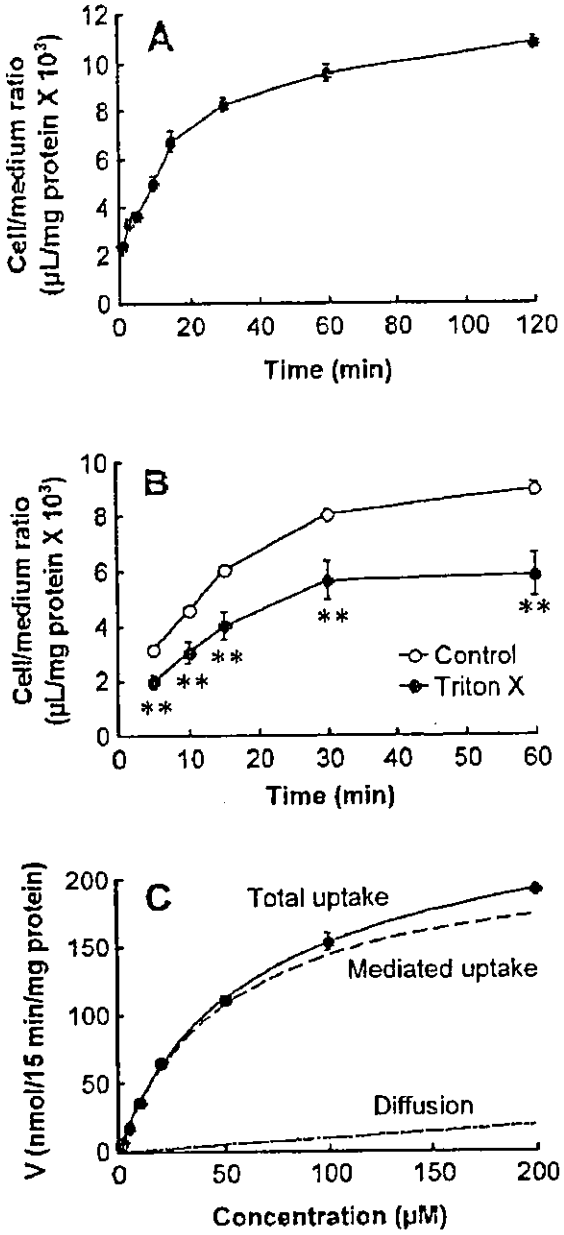

Fig. 2. Characteristics of quinacrine uptake by MBEC4 cells. Panel (A), time course of quinacrine (1 μM) uptake by MBEC4 cells. Panel (B), changes in the quinacrine (1 μM) uptake by MBEC4 cells exposed to 0.015% Triton X for 10 min before the uptake experiment. Panel (C), concentration-dependence of quinacrine uptake by MBEC4 cells. Initial uptake rates at various concentrations of quinacrine (1–200 μM) were measured at 37°C for 15 min. Curves for total, mediated, and diffusive uptake were drawn using the parameters obtained from nonlinear regression analysis (MULTI). Each point represents the mean ± SEM. (n = 4–20).** $P < 0.01$; significant difference from the control.

This document prepared for the sole and exclusive of Yasufumi Kataoka. Any unauthorized reproduction is strictly prohibited.

Table I. Effects of Various Compounds and Sodium-Replacement on Uptake of Quinacrine (1 μM) by MBEC4 Cells

Condition	Concentration	Cell/medium ratio (% of control)
NaN_3	10 mM	$67.2 \pm 3.03^{a,**}$
DNP	1 mM	$70.2 \pm 1.79^{a,**}$
4°C		$18.6 \pm 2.22^{a,**}$
FCCP	10 μM	$77.4 \pm 2.49^{a,**}$
Valinomycin	10 μM	97.2 ± 4.22^{a}
Amiloride	1 mM	97.4 ± 3.16^{a}
Tetraethylammonium	1 mM	$88.0 \pm 2.95^{b,**}$
	5 mM	$84.3 \pm 2.93^{b,**}$
	10 mM	$75.4 \pm 4.15^{b,**}$
Cimetidine	1 mM	$81.3 \pm 5.56^{c,**}$
	5 mM	$57.8 \pm 1.70^{c,**}$
	10 mM	$36.8 \pm 1.61^{c,**}$
Na^+ replacement with N-methylglucamine		104 ± 2.87^{d}

[a]MBEC4 cells were preincubated with NaN_3, DNP, FCCP, valinomycin, or amiloride for 10 min. Control values were $4.9 \pm 0.42 \times 10^3$ μL/mg protein. [b,c]Quinacrine uptake was measured by incubating MBEC4 cells with TEA or cimetidine. Control values were 4.1 ± 0.19 and $5.2 \pm 0.19 \times 10^3$ μL/mg protein, respectively.

[d]For investigation of the sodium dependency, quinacrine uptake was measured where Na^+ in the uptake buffer was replaced by N-methylglucamine. Control values were $3.6 \pm 0.22 \times 10^3$ μL/mg protein. Quinacrine uptake was measured at 37°C for 15 min. Values are expressed as % of control. Values are shown as means ± SEM ($n = 4$–20).

**$P < 0.01$; significant difference from the control.

(Fig. 3(B)). These findings demonstrated that quinacrine uptake by MBEC4 cells was pH-dependent. Pretreatment with 10 mM of NaN_3 inhibited quinacrine uptake at each pH used (Table II). Quinacrine uptake was not affected by 1 mM of amiloride (Table I). Therefore, quinacrine uptake was found to be unaffected by Na^+/H^+

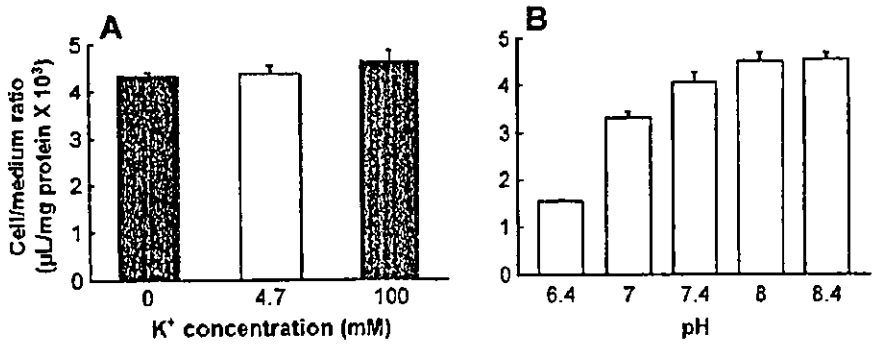

Fig. 3. Effects of the membrane potential (A) and pH (B) on the uptake of quinacrine (1 μM) by MBEC4 cells. Panel (A), effects of various concentrations of external potassium on quinacrine uptake: 0 mM (hyperpolarized), 4.7 mM (control), or 100 mM (depolarized). Panel (B), effects of various pH of the medium on quinacrine uptake. Quinacrine uptake was measured at 37°C for 15 min. Values are expressed as the cell-to-medium ratios. Values are shown as means ± SEM. ($n = 12$).

This document prepared for the sole and exclusive of Yasufumi Kataoka. Any unauthorized reproduction is strictly prohibited.

Table II. Effect of ATP Depletion on the Uptake of Quinacrine (1 μM) by MBEC4 Cells

	Cell/medium ratio (μL/mg protein $\times 10^3$)	
pH	Normal	ATP-depletion
6.4	1.61 ± 0.02	1.36 ± 0.03**
7.0	3.53 ± 0.14	3.28 ± 0.10
7.4	3.95 ± 0.32	3.20 ± 0.33*
8.0	4.71 ± 0.35	3.87 ± 0.30
8.4	4.77 ± 0.19	3.82 ± 0.22*

MBEC4 cells were preincubated with 10 mM NaN_3 for 10 min (ATP depletion). Quinacrine uptake was measured at 37°C for 15 min. Values are shown as means ± SEM ($n = 3$–8).
* $P < 0.05$, ** $P < 0.01$; significant difference from the control.

exchange. The effects of organic cations and P-gp inhibitors on quinacrine uptake were investigated. The organic cations including TEA (1-10 mM) and cimetidine (1–10 mM) significantly reduced quinacrine uptake by 12–25% and 19–65%, respectively (Table I). In the presence of cyclosporine (10 μM) or verapamil (20 μM), quinacrine uptake under the steady-state significantly increased by about 10% (Fig. 4).

To provide molecular evidence for the expression of OCTN1 in MBEC4 cells, RT-PCR was carried out (Fig. 5). With a primer pair specific for mouse OCTN1, RT-PCR with mRNA obtained from MBEC4 cells yielded a single product. The size of this product was the same as that expected from the primer positions in mouse OCTN1.

DISCUSSION

The BBB permeability coefficient of quinacrine, a candidate for the treatment of CJD, was much lower than that of Na-F, a BBB-impermeable marker, suggesting that

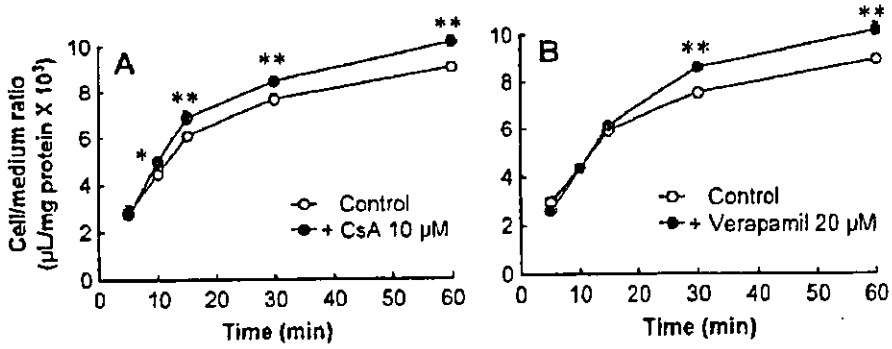

Fig. 4. Effects of 10 μM cyclosporine (A) and 20 μM verapamil (B) on uptake of quinacrine (1 μM) by MBEC4 cells. Quinacrine uptake was measured at 37°C in the absence and presence of cyclosporine or verapamil. Values are expressed as the cell-to-medium ratios. Values are shown as means ± SEM. ($n = 8$).

This document prepared for the sole and exclusive of Yasufumi Kataoka. Any unauthorized reproduction is strictly prohibited.

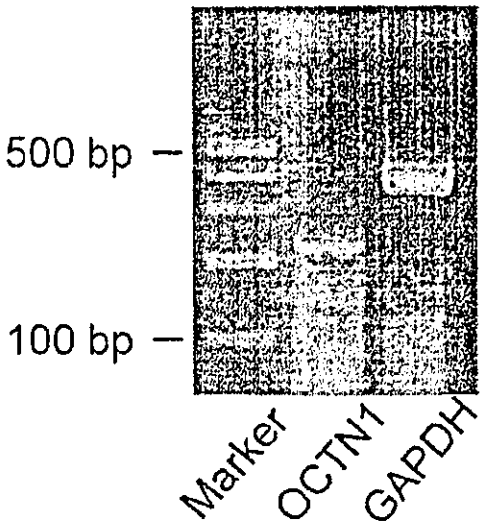

Fig. 5. Photograph showing OCTN1 expression in MBEC4 cells by RT-PCR. RNA samples from MBEC4 cells were used for RT-PCR with primer pairs specific for mouse OCTN1.

the permeability of quinacrine into the brain through the BBB is extremely low. To determine which machinery is involved in the low permeability of quinacrine across the BBB, we investigated the polarity of transcellular transport of quinacrine and the effects of P-gp inhibitors (cyclosporine and verapamil) on the BBB permeability of quinacrine. The basolateral-to-apical (brain-to-blood) transport of quinacrine across MBEC4 monolayer was greater than quinacrine transport in the opposite direction (Fig. 1(B)). Cyclosporine and verapamil increased the apical-to-basolateral (blood-to-brain) transport of quinacrine (Fig. 1(C)). Quinacrine uptake by MBEC4 cells under the steady-state was significantly increased by cyclosporine and verapamil (Fig. 4). These findings indicate the possible involvement of P-gp in the efflux transport of quinacrine. P-gp largely contributes to multidrug-resistance of the BBB in an ATP-dependent manner. This study provided controversial evidence that metabolic inhibitors or incubation at low temperature decreased quinacrine uptake (Table I). Quinacrine was actively and concentratively accumulated in MBEC4 cells. A large part of quinacrine is probably taken up via the saturable system, although quinacrine uptake was shown to have both saturable and nonsaturable pathways (Fig. 2(C)). Uptake of quinacrine by choroid plexus cells was organic cation-specific and energy-dependent (Miller *et al.*, 1999). In light of these findings, P-gp (an efflux system) and other influx transport system(s) are considered to mediate quinacrine transport into the brain.

We elucidated a role of the known organic cation transporters (OCT1, OCT2, OCT3, OCTN1, and OCTN2), and the specificity or driving force of those transporters in mediating quinacrine uptake by MBEC4 cells. Quinacrine uptake was significantly inhibited by various organic cations including TEA and cimetidine, which are known to be a substrate and an inhibitor of the organic cation transporters, respectively. Quinacrine uptake was insensitive to changes in the membrane potential (Fig. 3(A)) and strongly inhibited by lowering the external pH (Fig. 3(B)). These characteristics are distinct from those of the OCT1, OCT2, and OCT3, all of which

This document prepared for the sole and exclusive of Yasufumi Kataoka. Any unauthorized reproduction is strictly prohibited.

are dependent on the membrane potential (Gorboulev *et al.*, 1997; Grundemann *et al.*, 1994; Kekuda *et al.*, 1998). Considering quinacrine is an organic base, the pH-related decrease in quinacrine uptake may have resulted from an increase in the concentration of ionized quinacrine according to the pH partition theory. However, our data showing that quinacrine uptake by MBEC4 cells at each pH was inhibited by NaN_3 (Table II) suggest that a pH-sensitive transport system is involved in quinacrine uptake. Transport of quinacrine increased by elevating the outward H^+ gradient across the membrane. This finding indicates that quinacrine may be transported through MBEC4 cells by an H^+/quinacrine antiport. The activity of H^+/organic cation antiporter is regulated by pH or H^+ gradient as the driving force (Maegawa *et al.*, 1988). The H^+ gradient is formed by Na^+/H^+ exchange in the vicinity of the apical membrane of brain endothelial cells (Ennis *et al.*, 1996). The Na^+/H^+ exchange is, however, unlikely to participate in quinacrine uptake by MBEC4 cells, since Na^+-depletion and amiloride failed to reduce quinacrine uptake (Table I). OCTN1 is Na^+-independent organic cation transporter (Wu *et al.*, 2000). OCTN2 mediates uptake of L-carnitine and several organic cations in an Na^+-coupled and Na^+-independent manner, respectively (Wu *et al.*, 1999). OCTN1 is a pH-dependent organic cation transporter presumably energized by a proton antiport mechanism (Yabuuchi *et al.*, 1999). The characteristics of quinacrine transport obtained in this study are similar to those of OCTN1. Mouse OCTN1 is distributed in the brain, heart, and liver, and strongly expressed in the kidney (Tamai *et al.*, 2000). RT-PCR analysis of MBEC4 cells demonstrated the expression of OCTN1 (Fig. 5). Therefore, OCTN1 is suggested to be a potential transporter mediating quinacrine uptake by MBEC4 cells.

The BBB permeability of quinacrine was extremely low, although quinacrine was rapidly transported into the brain endothelial cells by the apical pH-dependent transport system. A weak organic base binds to a variety of polyanions including RNA, DNA, and ATP, and accumulates in the acidic intracellular compartments (Miller *et al.*, 1999). Quinacrine is distributed in the nucleus and vesicular compartment in the cytoplasm of choroid plexus cells (Miller *et al.*, 1999). In the brain endothelial cells, a large part of quinacrine was shown to be distributed and accumulated in the intracellular binding compartment (Fig. 2(B)). The resulting small part of quinacrine in the intracellular nonbinding compartment appears to contribute to the BBB permeability. The P-gp-mediated active efflux at the apical side of the plasma membrane and the large storage capacity in the cytoplasm are considered to restrict the entry of quinacrine into the brain. The mechanism involved in quinacrine transport at the basolateral side remains obscure.

In conclusion, quinacrine transport at the BBB is mediated by the influx and efflux transport systems. The influx of quinacrine is mediated by a pH-dependent and Na^+- and membrane potential-independent system, an OCTN1-like transporter. The efflux of quinacrine evoked by P-gp at the BBB restricts the entry of quinacrine into the brain. This phenomenon may be interpreted as lowering the therapeutic efficacy of quinacrine for CJD. This study may have clinical implications; quinacrine concentrations in the brain increased by P-gp modulators including verapamil may enhance the therapeutic efficacy of quinacrine for CJD.

This document prepared for the sole and exclusive of Yasufumi Kataoka. Any unauthorized reproduction is strictly prohibited.

ACKNOWLEDGMENTS

This work was supported in part by a Grant-in-Aid for Scientific Research ((B)(2) 14370789) from the Ministry of Education, Culture, Sports, Science, and Technology (MEXT), Japan.

REFERENCES

Bradford, M. M. (1976). A rapid and sensitive method for the quantitation of microgram quantities of protein utilizing the principle of protein dye binding. *Anal. Biochem.* **72**:248–254.

Chan, B. S., Satriano, J. A., Pucci, M., and Schuster, V. L. (1998). Mechanism of prostaglandin E_2 transport across the plasma membrane of HeLa cells and Xenopus oocytes expressing the prostaglandin transporter "PGT". *J. Biol. Chem.* **273**:6689–6697.

Dehouck, M.-P., Jolliet-Riant, P., Brée, F., Fruchart, J.-C., Cecchelli, R., and Tillement, J.-P. (1992). Drug transfer across the blood–brain barrier: Correlation between in vitro and in vivo models. *J. Neurochem.* **58**:1790–1797.

Ennis, S. R., Ren, X., and Betz, A. L. (1996). Mechanisms of sodium transport at the blood-brain barrier studied with in situ perfusion of rat brain *J. Neruochem.* **66**:756–763.

Follette, P. (2003). Prion disease treatment's early promise unravels. *Science* **299**:191–192.

Friedrich, A., George, R. L., Bridges, C. C., Prasad, P. D., and Ganapathy, V. (2001). Transport of cholin and its relationship to the expression of organic cation transporters in a rat brain microvessel cell line (RBE4). *Biochim. Biophys. Acta* **1512**:299–307.

Friedrich, A., Prasad, P. D., Freyer, D., Ganapathy, V., and Brust, P. (2003). Molecular cloning and functional characterization of the OCTN2 transporter at the RBE4 cells, an in vitro model of the blood-brain barrier. *Brain Res.* **968**:69–79.

Gorboulev, V., Ulzheimer, J. C., Akhoundova, A., Ulzheimer-Teuber, I., Karbach, U., Quester, S., Baumann, C., Lang, F., Busch, A. E., and Koepsell, H. (1997). Cloning and characterization of two human polyspecific organic cation transporters. *DNA Cell Biol.* **16**:871–881.

Grundemann, D., Gorboulev, V., Gambaryan, M., Vehyhl, M., and Koepsell, H. (1994). Drug excretion mediated by a new prototype of polyspecific transporter. *Nature* **372**:549–552.

Kekuda, R., Prasad, P. D., Wu, X., Wang, H., Fei, Y. J., Leibach, F. H., and Ganapathy, V. (1998). Cloning and functional characterization of a potential-sensitive, polyspecific organic cation transporter (OCT3) most abundantly expressed in placenta. *J. Biol. Chem.* **273**:15971–15979.

Koepsell, H. (1998). Organic cation transporters in intestine, kidney, liver, and brain. *Annu. Rev. Physiol.* **60**:243–266.

Korth, C., May, B. C. H., Cohen, F. E., and Prusiner, S. B. (2001). Acridine and phenothiazine derivatives as pharmacotherapeutics for prion disease. *Proc. Natl. Acad. Sci. U.S.A.* **98**:9836–9841.

Maegawa, H., Kato, M., Inui, K., and Hori, R. (1988). pH sensitivity of H^+/organic cation antiport system in rat renal brush-border membranes. *J. Biol. Chem.* **263**:11150–11154.

Miller, D. S., Villalobos, A. R., and Pritchard, J. B. (1999). Organic cation transport in rat choroid plexus cells studied by fluorescence microscopy. *Am. J. Physiol.* **276**:C955–C968.

Okuda, N., Saito, H., Urakami, Y., Takano, M., and Inui, K. I. (1996). cDNA cloning and functional expression of a novel rat kidney organic cation transporter. *Biochem. Biophys. Res. Commun.* **224**:500–507.

Sawada, N., Takanaga, H., Matsuo, H., Naito, M., Tsuruo, T., and Sawada, Y. (1999). Choline uptake by mouse brain capillary endothelial cells in culture. *J. Pharm. Pharmacol.* **51**:847–852.

Sweet, D. H., and Pritchard, J. (1999). rOCT2 is a basolateral potential-driven carrier, not an organic cation/proton exchanger. *Am. J. Physiol.* **277**:F890–F898.

Tamai, I., Ohashi, R., Nezu, J., Sai, Y., Kobayashi, D., Oku, A., Shimane, M., and Tsuji, A. (2000). Molecular and functional characterization of organic cation/carnitine transporter family in mice. *J. Biol. Chem.* **275**:40064–40072.

Tamai, I., Yabuuchi, H., Nezu, J., Sai, Y., Oku, A., Shimane, M., and Tsuji, A. (1997). Cloning and characterization of a novel human pH-dependent organic cation transporter, OCTN1. *FEBS Lett.* **419**:107–111.

Tatsuta, T., Naito, M., Mikami, K., and Tsuruo, T. (1994). Enhanced expression by the brain matrix of P-glycoprotein in brain capillary endothelial cells. *Cell Growth Differ.* **5**:1145–1152.

Tatsuta, T., Naito, M., Oh-hara, T., Sugawara, I., and Tsuruo, T. (1992). Functional involvement of P-glycoprotein in blood–brain barrier. *J. Biol. Chem.* **267**:20383–20391.

This document prepared for the sole and exclusive of Yasufumi Kataoka. Any unauthorized reproduction is strictly prohibited.

Wu, X., George, R. L., Huang, W., Wang, H., Conway, S. J., Leibach, F. H., and Ganapathy, V. (2000). Structural and functional characteristics and tissue distribution pattern of rat OCTN1, an organic cation transporter, cloned from placenta. *Biochim. Biophys. Acta* **1466**:315–327.

Wu, X., Huang, W., Prasad, P. D., Seth, P., Rajan, D. P., Leibach, F. H., Chen, J., Conway, S. J., and Ganapathy, V. (1999). Functional characteristics and tissue distribution pattern of organic cation transporter 2 (OCTN2), an organic cation/carnitine transporter. *J. Pharmacol. Exp. Ther.* **290**:1482–1492.

Wu, X., Prasad, P. D., Leibach, F. H., and Ganapathy, V. (1998). cDNA sequence, transport function, and genomic organization of human OCTN2, a new member of the organic cation transporter family. *Biochem. Biophys. Res. Commun.* **246**:589–595.

Yabuuchi, H., Tamai, I., Nezu, J., Sakamoto, K., Oku, A., Shimane, M., Sai, Y., and Tsuji, A. (1999). Novel membrane transporter OCTN1 mediates multispecific, bidirectional, and pH-dependent transport of organic cations. *J. Pharmacol. Exp. Ther.* **289**:768–773.

Yamaoka, K., Tanigawara, Y., Nakagawa, T., and Uno, T. (1981). A pharmacokinetic analysis program (MULTI) for microcomputer. *J. Pharmacobiodyn.* **4**:879–885.

This document prepared for the sole and exclusive of Yasufumi Kataoka. Any unauthorized reproduction is strictly prohibited.

Results of Quinacrine Administration to Patients with Creutzfeldt-Jakob Disease
Masashi Nakajima; Tatsuo Yamada; Tomohiko Kusuhara; Hisako Furukawa; Mitsuo T...
Dementia and Geriatric Cognitive Disorders; 2004; 17, 3; ProQuest Medical Library
pg. 158

Original Research Article

Dementia
and Geriatric
Cognitive Disorders

Dement Geriatr Cogn Disord 2004;17:158–163
DOI: 10.1159/000076350

Accepted: June 30, 2003
Published online: January 20, 2004

Results of Quinacrine Administration to Patients with Creutzfeldt-Jakob Disease

Masashi Nakajima[a] Tatsuo Yamada[a] Tomohiko Kusuhara[a]
Hisako Furukawa[b] Mitsuo Takahashi[b] Atsushi Yamauchi[c]
Yasufumi Kataoka[c]

Departments of [a]Neurology, [b]Clinical Pharmacology and [c]Pharmaceutical Care and Health Sciences, Fukuoka University, Fukuoka, Japan

Key Words
Creutzfeldt-Jakob disease · Prion · Quinacrine

Abstract
Several chemicals inhibit the accumulation of abnormal prion proteins in vitro. We administered one, the antimalarial agent quinacrine, to three patients with sporadic Creutzfeldt-Jakob disease (CJD) and to one with iatrogenic CJD. Quinacrine at 300 mg/day was given enterally for 3 months. Within 2 weeks of administration, the arousal level of the patient with akinetic mutism improved. The other 3 patients, insensible before treatment, had integrative responses such as eye contact or voluntary movement in response to verbal and/or visual stimuli restored. Clinical improvement was transient, lasting 1–2 months during treatment. Quinacrine was well tolerated, except for liver dysfunction and yellowish pigmentation. Although its antiprion activity in the human brain has yet to be proved, these modest effects of quinacrine suggest the possibility of using chemical intervention against prion diseases.

Copyright © 2004 S. Karger AG, Basel

Introduction

Creutzfeldt-Jakob disease (CJD), a prion-mediated disease in humans, is invariably fatal. Accumulation of the abnormal protease-resistant prion protein (PrP^{Sc}), formed posttranslationally from the normal endogenous protease-sensitive isoform (PrP^{c}), is a central event in CJD pathogenesis [1]. Recent outbreaks of a new variant of CJD in young people [2], and of iatrogenic CJD after cadaveric dura grafting [3], require that treatment be immediately available for dying humans. The antimalarial agent quinacrine has long been used to treat patients with malaria and giardiasis. Two recent reports found that quinacrine inhibits and eradicates PrP^{Sc} in scrapie-infected neuroblastoma cells [4, 5]. Korth et al. [5] found that of the acridine and phenothiazine derivatives they tested, quinacrine and chlorpromazine inhibited PrP^{Sc} accumulation, and they noted the importance of the aliphatic side chain on the middle ring moiety of tricyclic compounds. Quinacrine was 10 times more potent than chlorpromazine, its effective concentration for half-maximal inhibition (EC_{50}) of PrP^{Sc} formation being 300 n*M* [5] (400 n*M* in the report of Doh-Ura et al. [4]). After chronic oral administration of quinacrine to humans, its serum concentration exceeded 450 n*M* for a total dose of 4.5 g given over 6 days [6]. Quinacrine is also deposited in the brain [7], and the tissue to plasma concentration ratio

KARGER
Fax + 41 61 306 12 34
E-Mail karger@karger.ch
www.karger.com

© 2004 S. Karger AG, Basel
1420–8008/04/0173–0158$21.00/0

Accessible online at:
www.karger.com/dem

Masashi Nakajima, MD
Department of Neurology, Tokyo Rosai Hospital
4-13-21 Ohmori-minami, Ota-ku
Tokyo 143-0013 (Japan)
Tel. +81 3 3742 7301, Fax +81 3 3744 9310, E-Mail masashi@tokyob.rofuku.go.jp

Reproduced with permission of the copyright owner. Further reproduction prohibited without permission.

Table 1. Clinical findings before and after quinacrine treatment

Patient No./ age, years/ gender/Dx	Duration of illness	Before quinacrine administration		Feeding	After quinacrine administration		Duration of changes
		cognitive state	motility		cognitive state	motility	
1/46/M/ sCJD	11 months	akinetic mutism; roving eye movement; cortical blindness	eyes open to noxious stimuli; reflex myoclonus	NG tube	fixation of eyes	gaze oriented to the direction of a voice; decreased reflex myoclonus	from the 2nd to 5th week
2/58/M/ sCJD	2 months	alert; eye tracking for the object; startle response to visual, auditory and tactile stimuli; ignorance of object presented in the right visual field	withdrawal and purposeless movement; action myoclonus; paraplegia in flexion	NG tube	smiles at family members; eye tracking and startle response to an object presented in the right visual field	decreased action myoclonus	from the 6th day to the 6th week
3/61/F/ sCJD	2 months	alert; fearful, startle response; response to visual and auditory stimuli; right hemianopsia	withdrawal movement;	fed orally, or NG tube	increased eye contact with the examiner; laughter at visual and auditory stimuli	voluntary left arm movement and side-to-side head movement	from the 8th day to the 3rd week
4/58/F/ possibly iatrogenic CJD	6 years	alert; grimacing and moaning to noxious stimuli; listless to visual and auditory stimuli	palilalia; stereotyped limbs and orolingual movement; impossible to sit or stand up even with assistance	fed orally	apparent eye contact with people; laughter at visual and auditory stimuli; appropriate 'yes or no' to questions	able to sit up on a reclining chair	from the 2nd to 8th week

Dx = Diagnosis; NG = nasogastric.

is very high [8]. Its pharmacokinetics suggests that a concentration of quinacrine can be obtained in the human brain sufficient to inhibit abnormal prion accumulation, as shown in an in vitro experiment [4, 5].

Patients and Methods

Patients

Three patients with clinically probable sporadic CJD (sCJD; patients 1–3) and one with possible iatrogenic CJD which may have been transmitted by dura mater grafts (patient 4) were studied. Their ages, sex, duration of illness and status at the start of the study are given in table 1. These patients were admitted to Fukuoka University Hospital between October 2001 and February 2002. The three sCJD patients fulfilled the Masters', French and European criteria for probable CJD [9] and showed progressive dementia, myoclonus, visual or cerebellar signs, extrapyramidal signs, typical periodic sharp and slow wave complexes (PSWCs) on EEGs, and positive detection of CSF 14-3-3 proteins.

Patient 4 had undergone removal of a right cerebellopontine angle tumor and had had dura mater grafts in July 1991. She received a single brand of dura mater graft, LYODURA®, processed by B. Braun Melsungen AG before 1987, which brand was found to be responsible for a Japanese outbreak of iatrogenic CJD [3]. She developed progressive dementia in January 1996, became listless within 2 years, and was bedridden within 4 years of onset. Stereotyped repetitive limb movement (palikinesia) and a few patterns of simple sound repetition (palilalia) characterized her status. She moaned emotionally on manipulation of her limbs and had dysphasia, but swallowing was possible when fed. She had extrapyramidal rigidity and exaggerated tendon reflexes, but no ataxia, myoclonus, PSWCs or CSF 14-3-3 proteins. MRI showed diffuse cerebral atrophy. Nondegenerative dementias caused by anoxic brain damage or normal pressure hydrocephalus, and dementias of infectious, neoplastic, metabolic, nutritional or endocrine origin were excluded.

Methods

The four patients were administered 300 mg/day quinacrine enterally for 3 months. The study had been approved by our institution's ethics committee, and the patients' relatives had consented to the procedure. Quinacrine was given as 100 mg of powder in capsule form. It was administered orally 3 times a day after each meal, or through a nasogastric tube after being dissolved in water at 37°C. The patients' behavior and neurological examinations were videotaped every 2 weeks. Routine hematological and blood chemistry studies were done weekly, and EEGs were obtained every 2 weeks. Brain MRI that included diffusion-weighted (DW) images was done in the 4th and 12th weeks after treatment began. Quinacrine was withdrawn if major side effects such as convulsion, bone marrow suppression (white blood cell count <2,000/μl) or significant liver dysfunction (>5 times the normal upper limits for aspartate aminotransferase or alanine aminotransferase) occurred. In addition, if the patient's condition was complicated by infection, metabolic irregu-

Reproduced with permission of the copyright owner. Further reproduction prohibited without permission.

larities or gastrointestinal problems, quinacrine was withdrawn and readministered only when the condition had returned to normal. No other medicines were given during the period of quinacrine administration. The plasma concentration of quinacrine in the patients' blood samples was measured by high-performance liquid chromatography.

Results

Quinacrine was well tolerated by all the patients. Yellowish skin pigmentation invariably appeared 10–14 days after treatment began. Transaminase values were elevated in 3 of the 4 patients, but never reached 5 times the normal upper limits. Patients 1 and 2 had quinacrine withdrawn temporarily because of aspiration pneumonia, urinary tract infection or diarrhea, but both finally completed the 3-month treatment course.

Clinical Course

A change in cognitive state appeared during the first 2 weeks of treatment (table 1). Patient 1's unfocused, occasionally roving eyes (fig. 1a) became fixed (fig. 1b) and sometimes were oriented to the side of auditory stimuli (fig. 1c). When stimulated, patients 2 and 3 showed mitigation of irritable mood and the return of smiles or laughter. Patient 3, who had been apathetic (fig. 1d), made apparent eye contact with people (fig. 1e), turned her head from side to side in response to the examiner's position, and had purposeful, voluntary movement of the left arm (fig. 1f). Patient 4 also made eye contact with people and nonpathological laughter in response to stimuli was restored. She also nodded or shook her head, apparently indicating 'yes' or 'no', in response to simple verbal questions such as those about pain or thirst.

These changes in mood or cognitive function were invariably transient, lasting 2–8 weeks during the period of quinacrine administration, after which cognitive function gradually decreased to baseline levels. Due to the associated conditions described previously, quinacrine was temporarily withdrawn from patient 1 in the 5th and patient 2 in the 6th week. Both patients' conditions deteriorated to akinetic mutism that remained even after quinacrine was restarted. After 3–8 weeks of treatment, cognitive function in patients 3 and 4 had regressed with no predisposing factors.

EEG and MRI Findings

Patient 2 showed changes in both EEG and MRI findings, which may be associated with the clinical changes that occurred. Typical PSWCs in the severely suppressed background before treatment (fig. 2a) had become irregular slow activities with less periodicity and no suppression by day 16 of treatment (fig. 2b). Before treatment, DW-MRI detected high signals bilaterally in the corpus striatum and insular and cingulate gyri, as well as in the temporal and parietal lobes. The signal intensities in the temporal and parietal lobe lesions were higher on the left than the right (fig. 3a), at which time the patient did not respond to visual stimuli presented in the right visual field, but did respond to stimuli in the left visual field. Startle responses to threatening stimuli in the right visual field, which appeared on day 19 of treatment, lasted 2 weeks. DW-MRI on day 23 showed decreased high signal intensities in the left temporal and parietal lobes, whereas intensity remained high in the other regions (fig. 3b).

Fig. 1. Patients' appearances before (left) and after (right) quinacrine treatment. **a–c** Patient 1 had an apathetic appearance and unfocused, roving eye movements before treatment (**a**). After treatment, there was eye fixation (**b**) and gaze oriented to auditory stimulus (**c**). **d–f** Patient 3 was listless and apathetic before treatment (**d**). After treatment, she had a well-oriented facial expression (**e**) and purposeful limb movement (**f**).

Reproduced with permission of the copyright owner. Further reproduction prohibited without permission.

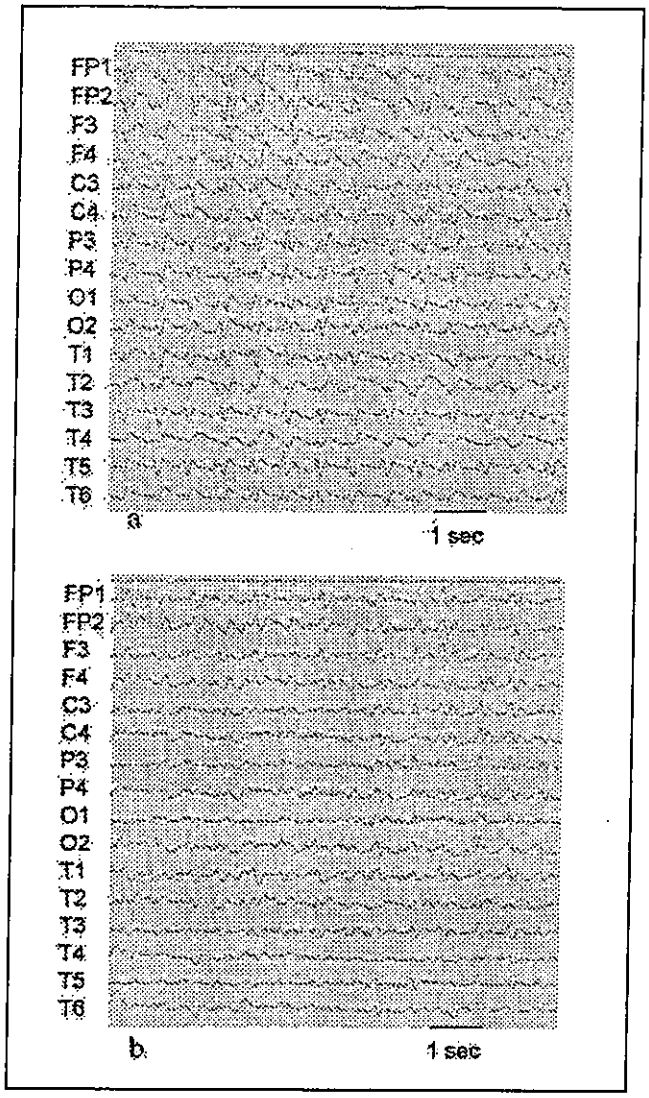

Fig. 2. Electroencephalograms for patient 2 before (**a**) and after (**b**) quinacrine treatment. PSWCs with totally suppressed background activities (**a**) were replaced by fewer periodic patterns and restored background activities after treatment (**b**).

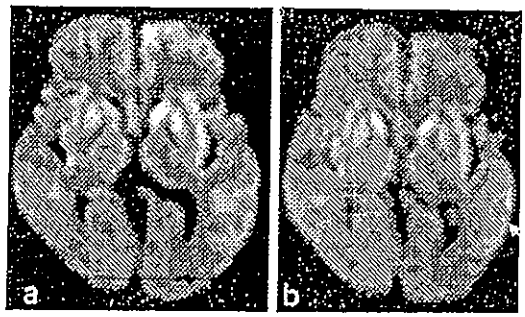

Fig. 3. DW-MRI of patient 2. The right side of each image corresponds to the left side of the brain. High signal intensities were present in the corpus striatum and insular and cingulate gyri on both sides, and in the parietal and temporal lobes before (**a**) and after (**b**) quinacrine treatment. In **b**, the high signal in the left temporoparietal lobes (arrow) is attenuated, whereas signals in the other regions remain unchanged.

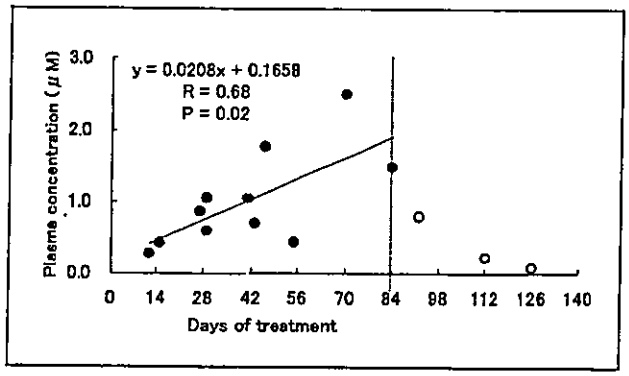

Fig. 4. Plasma concentrations of quinacrine during and after its administration. The concentration increased with the number of days of treatment. Quinacrine was still detectable in the plasma after drug discontinuation on day 84, indicating that it had accumulated in tissues.

Before treatment, patient 3 had high DW-MRI signals in the corpus striatum, cingulate gyrus and left parietal and temporal cortices. These had not changed by the 4th week of treatment, but they disappeared during the 12th week. The other two patients showed diffuse cerebral atrophy without high signals on DW-MRI, which findings did not change after treatment. On the EEGs, patient 1 had PSWCs in the suppressed background before treatment. These disappeared and were replaced by diffuse slow activities of 3–7 Hz during the 2nd week of treatment, but they returned during the 4th week and disappeared thereafter. Patient 3 had PSWCs superimposed on slow background activities, and patient 4 showed diffuse slowing with occasional alpha activities. These features remained unchanged after treatment.

Reproduced with permission of the copyright owner. Further reproduction prohibited without permission.

Plasma Concentration of Quinacrine

The plasma concentration of quinacrine increased with the length of administration (fig. 4). It reached 300 n*M* within 14 days and was as high as 2,500 n*M* near the end of the treatment period. Moreover, quinacrine was detectable in the patients' plasma 6 weeks after its discontinuation.

Discussion

In their search for potent agents to treat prion diseases, Doh-ura et al. [4] reported inhibition of PrP^{Sc} accumulation in scrapie-infected neuroblastoma cells by lysosomotropic agents, including quinacrine and cysteine protease inhibitors. These agents may interfere with the conversion of PrP^{c} to PrP^{Sc} at the plasma membrane or along an endocytotic pathway to the lysosomes. Recently, Collins et al. [10] reported that quinacrine did not prolong survival in a murine CJD model. Results of animal experiments, however, depend on the animal species and prion strain. Subcutaneous quinacrine administration prolonged the survival of transgenic mice inoculated with 263K scrapie agents into the brain [Doh-ura, pers. commun.].

We studied four patients, of whom three had clinically probable sCJD and one possibly iatrogenic CJD. All four had improved arousal levels after quinacrine treatment. Other changes in global brain function included decreased frequencies of reflex or action myoclonus (patients 1 and 2) and startle response (patients 2 and 3), and mitigation of the hyperkinetic state (patient 4). Focal brain functions restored were nonpathological laughter (patients 2–4), visual field (patient 2) and voluntary movement (patient 3). These changes might have been due to factors other than quinacrine, e.g. encouragement of contact by family members or caregivers, but this could be excluded for two reasons. Firstly, in Japan, intensive care is customarily given to severely disabled patients who have definitely poor prognoses. As in the case of patient 1, tube feeding is usually initiated and continued for irreversibly disabled patients because family members will not accept the cessation of feeding. The contact provided by family members and caregivers did not change after quinacrine treatment was begun in the present study. Secondly, the changes seen after treatment were transient, lasting 2–8 weeks. Thereafter, the patients' conditions regressed, even during quinacrine administration.

Of the three patients with clinically probable sCJD, transient improvement occurred not only in patients 2 and 3, who were in the early stage, but also in patient 1, who was in the terminal, akinetic mutism stage. This last patient had an improved arousal level associated with directed fixation of the eyes (fig. 1a–c) attributable to the function of the brainstem reticular formation, a structure relatively preserved in the classic, Heidenhain variant of sCJD [11]. The most marked change, seen in patient 2, was the restored response to objects presented in the right visual field. This change was accompanied by decreased DW-MRI signal intensities in the left temporal and parietal lobes. DW-MRI is a new technique that noninvasively images molecular water proton diffusion processes that occur on a micrometer scale [12]. Mittal et al. [13] reported that in CJD, the high-intensity signal areas seen in DW-MRI are correlated with a high degree of spongiform change. They speculated that these changes are the result of the microvacuolation of neuritic processes, heralding spongiform degeneration. Of our four patients, the two who were in the early stage of illness had high signals on DW-MRI that lasted for 2–3 months but which had disappeared 5 months into the illness. Although the exact mechanism is unknown, the immature attenuation of the high signals in the temporal and parietal lobes, which was correlated with clinical changes in patient 2, suggests that the high DW-MRI signals in CJD may represent reversible changes. Decreases in the action myoclonus and startle response in patient 2 were accompanied by decreased PSWCs and increased EEG background activity. These EEG findings suggest that mitigation of the irritable state, which produced a calm appearance, was due to improved cortical function and not to deterioration.

Cognitive function was restored temporarily in patient 4, who had an unusually prolonged course. She may have received contaminated cadaveric dura mater before onset, and her incubation period of 66 months compares with the incubation periods of other Japanese patients (mean incubation period 89 ± 44 months, range 16–193 months) during the CJD outbreak [3]. She had rapidly progressive dementia during the first 2 years of her total, prolonged 6-year course. Some Japanese patients with dura mater-associated CJD may have a clinically variant, longer duration of illness, characterized pathologically by florid-type plaques [14]. The diagnosis in that patient's case has had to be postponed, but quinacrine treatment appears to be beneficial for patients with rapidly progressive dementia and prolonged survival.

Whether the changes found are due to the antiprion effect of quinacrine, as reported in in vitro experiments, is unknown. Therapeutic doses of quinacrine are known to cause psychomotor hyperactivity. The incidence of quinacrine psychosis is reported to be 0.9–4 per 1,000 persons

Reproduced with permission of the copyright owner. Further reproduction prohibited without permission.

[15]. Engel et al. [16] administered 2.1–2.8 g of quinacrine to 5 healthy individuals over a 10-day period, doses sufficient to obtain plasma levels exceeding 250 n*M*. Their subjects had various degrees of psychomotor hyperactivity and increases in EEG frequencies. The EEG changes occurred at plasma quinacrine levels of 75–100 n*M* and continued for up to 8 days after discontinuation of the drug. The increased arousal levels in our patients, therefore, may be attributable to the cortical stimulation action of quinacrine, but the mechanism of its direct effect on the central nervous system has yet to be determined.

The plasma concentrations of quinacrine in our patients suggest that a therapeutic dose of 300 mg/day quinacrine may reach the EC_{50} of PrP^{Sc} formation, i.e. 300–400 n*M*, in brain tissues. Quinacrine accumulates progressively in tissues when administered chronically [7]. The lowest concentrations are in the brain, heart and skeletal muscle [7], but tissue to plasma concentration ratios may be very high, as in dog skeletal muscle [8]. The clinical changes in our patients occurred from the 2nd to 8th week of administration, and the plasma concentrations ranged from 300 to 1,000 n*M*. Those concentrations would be sufficient for the drug's accumulation in brain tissues as well as for its action either as a direct cortical stimulant or through its antiprion activity. Cognitive state regression during quinacrine treatment may be due to its toxicity on the brain [6]. We believe that the quinacrine dose should be decreased after the initial loading dose and the plasma concentration of the drug monitored. Although its effectiveness is limited in terms of extent and duration, our findings support undertaking a clinical trial of quinacrine and the search for other chemicals that prevent the accumulation of, or conformational changes in, prion proteins.

Acknowledgment

This study was supported by Research Grant No. 13080901 from the Ministry of Health, Labor and Welfare of Japan.

References

1 Prusiner SB, Hsiao KK: Human prion diseases. Ann Neurol 1994;35:385–395.
2 Will RG, Ironside JW, Zeidler M, Cousens SN, Estibeiro K, Alperovitch A, Poser S, Pocchiari M, Hofman A, Smith PG: A new variant of Creutzfeldt-Jakob disease in the UK. Lancet 1996;347:921–925.
3 Creutzfeldt-Jakob disease associated with cadaveric dura mater grafts – Japan, January 1979–May 1996. MMWR Morb Mortal Wkly Rep 1997;46:1066–1069.
4 Doh-Ura K, Iwaki T, Caughey B: Lysosomotropic agents and cysteine protease inhibitors inhibit scrapie-associated prion protein accumulation. J Virol 2000;74:4894–4897.
5 Korth C, May BC, Cohen FE, Prusiner SB: Acridine and phenothiazine derivatives as pharmacotherapeutics for prion disease. Proc Natl Acad Sci USA 2001;98:9836–9841.
6 Lidz T, Kahn RL: Toxicity of quinacrine (atabrine) for the central nervous system. III. An experimental study on human subjects. Arch Neurol Psychiatry 1946;56:284–299.
7 Rolls IM: Drugs used in the chemotherapy of helminthiasis; in Goodman LS, Gillman A (eds): Pharmacological Basis of Therapeutics, ed 5. New York, Macmillan, 1975, pp 1080–1094.
8 Shannon JA, Earle DP, Brodie BB, Taggart JV, Berliner RW: The pharmacological basis for the rational use of atabrine in the treatment of malaria. J Pharmacol Exp Ther 1944;81:307–330.
9 Brandel J-P, Delasnerie-Laupêtre N, Laplanche J-L, Hauw J-J, Alpérovitch A: Diagnosis of Creutzfeldt-Jakob disease: Effect of clinical criteria on incidence estimates. Neurology 2000;54:1095–1099.
10 Collins SJ, Lewis V, Brazier M, Hill AF, Fletcher A, Masters C: Quinacrine does not prolong survival in a murine Creutzfeldt-Jakob disease model. Ann Neurol 2002;52:503–506.
11 Parchi P, Giese A, Capellari S, Brown P, Schulz-Schaeffer W, Windl O, Zerr I, Budka H, Kopp N, Piccardo P, Poser S, Rojiani A, Streichemberger N, Julien J, Vital C, Ghetti B, Gambetti P, Kretzschmar H: Classification of sporadic Creutzfeldt-Jacob disease based on molecular and phenotypic analysis of 300 subjects. Ann Neurol 1999;46:224–233.
12 Moseley ME, Butts K: Diffusion and perfusion; in Stark DD, Bradley WG Jr (eds): Magnetic Resonance Imaging. St. Louis, Mosby, 1999, p 1515.
13 Mittal S, Farmer P, Kalina P, Kingsley PB, Halperin J: Correlation of diffusion-weighted magnetic resonance imaging with neuropathology in Creutzfeldt-Jakob disease. Arch Neurol 2002;59:128–134.
14 Shimizu S, Hoshi K, Muramoto T, Homma M, Ironside JW, Kuzuhara S, Sato T, Yamamoto T, Kitamoto T: Creutzfeldt-Jakob disease with florid-type plaques after cadaveric dura mater grafting. Arch Neurol 1999;56:357–362.
15 Lindenmayer J-P, Vargas P: Toxic psychosis following use of quinacrine. J Clin Psychiatry 1981;42:162–164.
16 Engel GL, Romano J, Ferris EB: Effect of quinacrine (atabrine) on the central nervous system, clinical and electroencephalographic studies. Arch Neurol Psychiatry 1947;58:337–350.

Reproduced with permission of the copyright owner. Further reproduction prohibited without permission.

薬理と治療（JPT）
JAPANESE PHARMACOLOGY & THERAPEUTICS（国際文献略号 *Jpn Pharmacol Ther*）
2004年12月25日発行　vol.32 supplement　別刷

24. 肝シヌソイド側における異物排泄トランスポーター（MRP4）の機能解析

東京大学大学院薬学系研究科　分子薬物動態学教室

楠原洋之　竹内健二　杉山雄一

ライフサイエンス出版

TEL（03）3664-7900（代表）

【禁 無断転載・複製】

24. 肝シヌソイド側における異物排泄トランスポーター（MRP4）の機能解析

東京大学大学院薬学系研究科　分子薬物動態学教室

楠原洋之　竹内健二　杉山雄一

Functional Characterization of MRP4

Hiroyuki Kusuhara, Kenji Takeuchi, Yuichi Sugiyama

The Graduate School of Pharmaceutical Sciences, the University of Tokyo

はじめに

肝臓は異物排泄臓器として重要な組織である。薬物の肝胆系輸送には種々のトランスポーターが関与していることが明らかにされている。胆管側膜での排泄過程では，細胞質側ドメインにヌクレオチド結合ドメインをもつABCトランスポーターが種々同定されている[1,2]。これらは，ATPの加水分解と共役した一次性能動輸送により，基質化合物を胆汁中へと排泄する。グルクロン酸，グルタチオン抱合体，両親媒性の有機アニオンを基質とするmultidrug resistance associated protein 2（MRP2/*ABCC2*），脂溶性の高いカチオン・中性薬物を基質とするP-糖タンパク（P-gp/*ABCB1*）が同定されている。MRP2は異物排泄のほか，グルタチオンの胆汁排泄にも関与しており，胆汁酸を分泌するBile Sale Export Pump（BSEP/*ABCB11*）と並んで，胆汁流を生成する重要な役割を果たす。

近年，Breast Cancer Resistance protein（BCRP/*ABCG2*）も同じく胆管側膜に局在することが示されている[3,4]。BCRPはP-gpやMRP2，BSEPとは異なり，N末側にヌクレオチド結合ドメインを有し，6回膜貫通領域で構成されるが，生理的にはホモダイマーを構成して，薬物排出ポンプとして機能する[5]。BCRPは抗癌剤のほか，硫酸抱合体，シメチジンや食品中に含まれる発癌剤PhIPも基質とする[5~7]。遺伝子欠損マウスではPhIP[8]や抗がん剤methotrexate[9]の胆汁排泄が低下することから，MRP2，P-gpとともに胆管側の異物排泄ポンプとしての重要性が明らかにされつつある。

肝シヌソイド側膜にもABCトランスポーターは発現していることが見いだされており，MRP familyに属する分子種であるMRP3，-4，-6が同定されている。MRP3は，MRP2を先天的に欠損した変異動物（Eisai Hyperbilirubinemic rat：EHBR）で，肝臓での発現が誘導されていることから見いだされたABCトランスポーターである[10]。MRP3は正常ラットの肝臓ではほとんど発現していないが，EHBRや肝内性胆汁うっ滞を引き起こすα-naphthylisothiocyanateやCytochrome P-450を誘導するphenobarbital，bilirubinを投与したラットではその発現が誘導される[11]。MRP3の基質にはグルクロン酸抱合体が含まれ，さらに胆汁酸も基質とすることが明らかにされている[12,13]。phenobarbital投与時，またEHBRでシヌソイド側でのtaurocholateの排出能力とMRP3の発現量には相関があり[14]，誘導時にMRP3

がシヌソイド側における排出ポンプとして働き，抱合代謝物や胆汁酸など異物の蓄積を防いでいることが示唆される。MRP6は，皮膚真皮における弾性線維の変性とカルシウム沈着で特徴づけられる弾性線維性仮性黄色種（pseudoxanthoma elasticum：PXE）の原因遺伝子と考えられている[15]。PXEは視野狭窄，皮膚障害，血管でのアテローム硬化症などの病変を伴うことが知られていたが，その原因遺伝子は長きにわたり明らかとなっていなかった。ポジショナルクローニング法によりその原因遺伝子が探索され，PXEの患者では，MRP6に変異がはいっていることが見いだされた。エンドセリンA受容体拮抗薬であるBQ-123やグルタチオン抱合体のLTC4，N-ehylmaleimide S-glutathione，グルクロン酸抱合体estradiol 17β glucuronideを基質とするもの[16,17]，病態と直接関連のある内因性基質の同定には至っていない。

MRP4は核酸アナログである抗ウィルス薬である9-(2-phosphonylmethoxyethul) adenineの排泄に関与し，MRP4過剰発現細胞はこれら核酸アナログに対し耐性を示す[18]。核酸アナログ以外に，DHEASやestradiol 17β glucuronideなどステロイドの抱合体やprostaglandinなども基質として輸送する[19~21]。さらに，グルタチオン存在下では，taurocholateも輸送基質とすることが報告されている[22]。肝臓ではシヌソイド側膜に局在していることから[22]，正常時にtaurocholateをはじめとする基質化合物のシヌソイド側における排出ポンプとして機能していることが示唆されている。

本研究では，肝胆管側膜と肝シヌソイド側膜に発現していることが近年見いだされたMRP4とBCRPについてアデノウィルスを用いた遺伝子発現系を構築し，その基質選択性について検討を加えた。

I 実験方法

1 化合物

[^{3}H]Dehydroepiandrosterone sulfate (DHEAS；79.1 Ci/mmol)，[^{3}H]p-aminohippuric acid (PAH；4.22 Ci/mmol) および[^{3}H]estrone sulfate (E_1S；46 Ci/mmol) はPerkinElmer Life Science (Boston, MA) から購入した。[^{3}H]ochratoxinA (21.3 Ci/mmol)，[^{14}C]uric acid (53 mCi/mmol)，[^{3}H]xanthine (20 Ci/mmol)，[^{3}H]hypoxanthine (20 Ci/mmol)，[^{3}H]cAMP (17 Ci/mmol) および[^{3}H]cGMP (2.4 Ci/mmol) はMoravek (Brea, CA) から購入した。[^{3}H]Pravastatin (45.5 Ci/mmol) およびその非標識体は三共㈱に供与していただいた。

2 Western Blot Analyses

Anti-hMRP4 (PC-063) およびanti-hBCRP (BXP-21) モノクローナル抗体はKamiya Biomedicalから購入した。膜ベシクルを3×SDSサンプルバッファー (New England BioLabs, Beverly, MA) に溶解後，3分間ボイルし，10% SDS-polyacrylamideゲル電気泳動を行った。泳動後，蛋白質をゲルからニトロセルロース膜 (Millipore, Bedford, MA) に転写した (15 V for 1時間)。転写後，PBS+5%スキムミルクで1時間振盪後，一次抗体を添加し，さらに1時間室温で振盪した。ニトロセルロース膜をPBS+0.1% Tween-20で洗浄後，Alexa Fluor 680 anti-mouse IgG (Molecular Probes, Inc. Eugene, OR) により検出した。

3 hMRP4 cDNAのクローニング

hMRP4 cDNAは，ヒト腎臓RNA (STRATAGENE) からRT-PCRにより単離した。PCRプライマーは，GenBank accession number AF071202の配列に基づいて設計し，センス鎖5′-AAGATGCTGCCCGTGTACCA-3′とし，アンチセンス鎖は5′-TGTCAAGTCCGTTCCGAAGG-3′とした。単離したcDNAは，3532番目のTがGであった。このことにより，1139番目のアミノ酸がAsnからLysに変異していた。Direct Sequenceにより，この変異は鋳型としたヒト腎臓RNA由来であった。

4 hMRP4を導入したアデノウィルスの作製

単離したヒトMRP4 cDNAをpShuttle vector plasmid (ApaI, KpnIサイト) に組込み，さらにAdeno-X™ Expression System (BD Biosciences, Palo Alto, CA) を用いて，Adeno-XTM Viral DNAへと組込んだ。hMRP4-組込みアデノウィルスを作製するため，pAd-hMRP4をPacIで処理後，HEK293 cellsにFuGENE6 (Roche Diagnostics Corporation, Indianapolis, IN) を用いて導入した。Recombinant viruses of hMRP4 and hBCRPはCsCl密度勾配遠心法により精製し，ストック溶液 (10 mM Tris (pH 7.5)，1 mM

MgCl2 および 10% glycerol）に懸濁後，−80℃ で保存した。ヒト BCRP については，既報[23]であるので，詳細はそちらを参照していただきたい。

5 膜ベシクルの調製

常法に従って，膜ベシクルを調製した[23]。ヒト胎児腎由来細胞（HEK293，2×10^6）を，15 cm シャーレ上で培養した。72 時間後，細胞を hMRP4-or hBCRP 組換えアデノウィルスを，1×10^8 pfu per plate で感染させた。ネガティブコントロールとして，GFP 組換えアデノウィルス（pAd-GFP）を感染させた。感染後 48 時間に，細胞を回収した。細胞は，40 倍の低張バッファー（1 mM Tris-HCl, 0.1 mM EDTA, pH 7.4, 4℃）にて，1 時間振盪し，破砕した。ホモジネートを 100000 g，30 分間遠心後，ペレットを 10 mL 等張 TS バッファー（10 mM Tris-HCl, 250 mM sucrose, pH 7.4 at 4℃）に懸濁し，Dounce B homogenizer（glass/glass, tight pestle, 30 strokes）でホモジナイズした。得られた粗膜分画を，38%（w/v）スクロース溶液（5 mM Tris-HEPES, pH 7.4, 4℃）にのせ，280000 g で 45 分間遠心した。境界面を回収し，23 mL の TS バッファーに懸濁後，100000 g で 30 分間遠心した。ペレットを 400 μL の TS バッファーに懸濁し，27-gauge の注射針を 30 回通すことでベシクル化した。ベシクルは−80℃ にて保存した。

6 膜ベシクルを用いた輸送実験

トランスポートバッファー（10 mM Tris, 250 mM sucrose and 10 mM $MgCl_2$. $6H_2O$, pH 7.4）に，基質，ATP（5 mM）およびその再生系（10 mM creatine phosphate and 100 g/L creatine phosphokinase）を添加した。37℃ にて，3 分間インキュベーションした後，膜ベシクルを添加し，実験開始とした。一定時間インキュベーション後，氷中においた 1 mL バッファー（250 mM sucrose, 100 mM NaCl, 10 mM Tris-HCl, pH 7.4）を加え反応を停止させ，そのうち 900 μL を 0.45 μm HA フィルター（Millipore Corp., Bedford, MA）にアプライし，濾過する。さらに，5 mL のバッファーで 2 回洗浄する。フィルター上の放射活性（LS 6000SE, Beckman Instruments, Fullerton, CA）を用いて測定した。ベシクルへの取込みは，トランスポートバッファー中の放射活性で補正した。

II 結果および考察

Western blot 法により，MRP4 組換え型アデノウィルスを感染させた HEK293 から調製したベシクル（MRP4-HEK）に，約 190 kDa の位置に MRP4 の発現を確認した。このベシクルを用いて，種々化合物について ATP 依存的な輸送活性の比較を行った。BCRP 発現ベシクルについても，BCRP 組換え型アデノウィルスを感染させた HEK293 から調製した[23]。

BCRP-HEK では，DHEAS（K_m=30 μM），estrone sulfate（E1S）などステロイド抱合体，pravastatin や，尿中に主として排泄される有機アニオンである ochratoxin A（K_m=270 μM），PAH（K_m=5.6 mM），cAMP（K_m=3.1 mM），cGMP（K_m=6.0 mM），methotrexate（K_m=5.2 mM）や，xanthine, hypoxanthine, urate（K_m=2.5 mM）など核酸代謝物など非常に広範な化合物の ATP 依存的な輸送活性を検出することができた。PAH をはじめとして腎排泄型の有機アニオンに対する K_m 値は，ステロイド抱合体に比べて大きい値を示し，E1S, ochratoxinA が DHEAS の輸送活性と同程度であるが，他の基質化合物については，20 分の 1 以下の輸送活性であった。

MRP4-HEK では，DHEAS（K_m=2.7 μM）のほか，PAH（K_m=738 μM），methotrexate（K_m=100 μM），pravastatin, cGMP, xanthine の輸送活性は検出できたのに対して，E_1S, ochratoxin A, cAMP, hypoxanthine では GFP-HEK に比較して，有意な取込みを検出できなかった。ochratoxin A が DHEAS の 6 分の 1 程度の輸送活性であるが，他の基質については DHEAS の 20 分の 1 以下であった。

DHEAS に比較すると輸送活性は低いながらも，MRP4 と BCRP が両親媒性の有機アニオンのほか，腎排泄型の有機アニオンも基質とするなど，幅広い基質選択性を有していることが明らかとなった。基質化合物には一部重複もみられたが，DHEAS や PAH, methotrexate は BCRP よりも MRP4 に対して高い親和性を示し，E_1S など BCRP のみで輸送が検出された化合物も見いだされた。

おわりに

本研究では，MRP4 と BCRP の遺伝子発現系を用いて，両トランスポーターの基質化合物の探索を行い，特に腎排泄型の有機アニオンも基質とすることを見いだした。MRP4 と BCRP は肝シヌソイド側，胆管側膜に発現しているが，今回見いだした基質の肝内動態にどのように関連しているのか，さらに検討を進める必要がある。最近，BCRP[3] と MRP4[24] を欠損したマウスも作出されており，こうしたマウスを用いた *in vivo/in situ* での解析により，それぞれのトランスポーターの役割は明確にされるであろう。

また，肝臓以外の臓器として，MRP4 は肝臓以外にも，腎近位尿細管（刷子縁膜）[21]，脳毛細血管内皮細胞（管腔側）[24] に，BCRP は小腸上皮細胞（刷子縁膜）[3,4]，脳毛細血管内皮細胞（管腔側）[25] のほか，マウスでは腎（刷子縁膜）[3] に発現していることから，これらの組織において異物排泄システムとしての役割についても今後検討していく必要がある。

BCRP については，141 番目のアミノ酸残基に遺伝子多型（Gln141Lys）が存在し，変異型（141Lys）では，BCRP のタンパクとしての発現量は低下する[23,26]。さらに，日本人では頻度高く，Allele 頻度としては約 30% に達する[26]。この変異をヘテロで有する患者では，抗がん剤 diflomotecan の静脈内投与後の血中消失の遅延が報告されており[27]，薬剤感受性の個人差を決定する要因として注目されている。MRP4 についても，体内動態における役割を明らかにするとともに，遺伝子多型を解析し，薬剤感受性における個人差の要因としてどの程度重要であるのか解析を進めていくことが必要である。

【謝辞】 本研究を遂行することにあたり，非標識体の pravastatin ならびに標識体の pravastatin を御供与していただきました三共㈱に深謝いたします。

文　献

1) Meier PJ, Stieger B. Bile salt transporters. Annu Rev Physiol 2002；64：635-61.
2) Faber KN, Muller M, Jansen PL. Drug transport proteins in the liver. Adv Drug Deliv Rev 2003；55：107-24.
3) Jonker JW, Buitelaar M, Wagenaar E, Van Der Valk MA, Scheffer GL, Scheper RJ, et al. The breast cancer resistance protein protects against a major chlorophyll-derived dietary phototoxin and protoporphyria. Proc Natl Acad Sci U S A 2002；99：15649-54.
4) Maliepaard M, Scheffer GL, Faneyte IF, van Gastelen MA, Pijnenborg AC, Schinkel AH, et al. Subcellular localization and distribution of the breast cancer resistance protein transporter in normal human tissues. Cancer Res 2001；61：3458-64.
5) Doyle LA, Ross DD. Multidrug resistance mediated by the breast cancer resistance protein BCRP (ABCG2). Oncogene 2003；22：7340-58.
6) Suzuki M, Suzuki, H, Sugimoto Y, Sugiyama Y. ABCG2 transports sulfated conjugates of steroids and xenobiotics. J Biol Chem 2003；278：22644-9.
7) Pavek P, Merino G, Wagenaar E, Bolscher E, Novotna M, Jonker JW, et al. Human Breast Cancer Resistance Protein (BCRP/ABCG2)：interactions with steroid drugs, hormones, the dietary carcinogen PhIP, and transport of cimetidine. J Pharmacol Exp Ther. (In press)
8) van Herwaarden AE, Jonker JW, Wagenaar E, Brinkhuis RF, Schellens JH, Beijnen JH, et al. The breast cancer resistance protein (Bcrp1/Abcg2) restricts exposure to the dietary carcinogen 2-amino-1-methyl-6-phenylimidazo [4,5-b] pyridine. Cancer Res 2003；63：6447-52.
9) Breedveld P, Zelcer N, Pluim D, Sonmezer O, Tibben MM, Beijnen JH, et al. Mechanism of the pharmacokinetic interaction between methotrexate and benzimidazoles：potential role for breast cancer resistance protein in clinical drug-drug interactions. Cancer Res 2004；64：5804-11.
10) Hirohashi T, Suzuki H, Ito K, Ogawa K, Kume K, Shimizu T, et al. Hepatic expression of multidrug resistance-associated protein-like proteins maintained in eisai hyperbilirubinemic rats. Mol Pharmacol 1998；53：1068-75.
11) Ogawa K, Suzuki H, Hirohashi T, Ishikawa T, Meier PJ, Hirose K, et al. Characterization of inducible nature of MRP3 in rat liver. Am J Physiol Gastrointest Liver Physiol 2000；278：G438-46.
12) Hirohashi T, Suzuki H, Takikawa H, Sugiyama Y. ATP-dependent transport of bile salts by rat multidrug resistance-associated protein 3 (Mrp3). J Biol Chem 2000；275：2905-10.
13) Hirohashi T, Suzuki H, Sugiyama Y. Characterization of the transport properties of cloned rat multidrug resistance-associated protein 3 (MRP3). J Biol Chem 1999；274：15181-5.
14) Akita H, Suzuki H, Sugiyama Y. Sinusoidal efflux of taurocholate correlates with the hepatic expression level of Mrp3. Biochem Biophys Res Commun 2002；299：681-7.
15) Le Saux O, Urban Z, Tschuch C, Csiszar K, Bacchelli B, Quaglino D, et al. Mutations in a gene encoding an ABC

transporter cause pseudoxanthoma elasticum. Nat Genet 2000 ; 25 : 223-7.
16) Ilias A, Urban Z, Seidl TL, Le Saux O, Sinko E, Boyd CD, et al. Loss of ATP-dependent transport activity in pseudoxanthoma elasticum-associated mutants of human ABCC6 (MRP6). J Biol Chem 2002 ; 277 : 16860-7.
17) Madon J, Hagenbuch B, Landmann L, Meier PJ, Stieger B. Transport function and hepatocellular localization of mrp6 in rat liver. Mol Pharmacol 2000 ; 57 : 634-41.
18) Schuetz JD, Connelly MC, Sun D, Paibir SG, Flynn PM, Srinivas RV, et al. MRP4 : A previously unidentified factor in resistance to nucleoside-based antiviral drugs. Nat Med 1999 ; 5 : 1048-51.
19) Reid G, Wielinga P, Zelcer N, van der Heijden I, Kuil A, de Haas M, et al. The human multidrug resistance protein MRP4 functions as a prostaglandin efflux transporter and is inhibited by nonsteroidal antiinflammatory drugs. Proc Natl Acad Sci U S A 2003 ; 100 : 9244-9.
20) Zelcer N, Reid G, Wielinga P, Kuil A, van der Heijden I, Schuetz JD, et al. Steroid and bile acid conjugates are substrates of human multidrug-resistance protein (MRP) 4 (ATP-binding cassette C4). Biochem J 2003 ; 371 : 361-7.
21) van Aubel RA, Smeets PH, Peters JG, Bindels RJ, Russel FG. The MRP4/ABCC4 gene encodes a novel apical organic anion transporter in human kidney proximal tubules : putative efflux pump for urinary cAMP and cGMP. J Am Soc Nephrol 2002 ; 13 : 595-603.
22) Rius M, Nies AT, Hummel-Eisenbeiss J, Jedlitschky G, Keppler D. Cotransport of reduced glutathione with bile salts by MRP4(ABCC4) localized to the basolateral hepatocyte membrane. Hepatology 2003 ; 38 : 374-84.
23) Kondo C, Suzuki H, Itoda M, Ozawa S, Sawada J, Kobayashi D, et al. Functional analysis of SNPs variants of BCRP/ABCG2. Pharm Res 2004 ; 21 : 1895-903.
24) Leggas M, Adachi M, Scheffer GL, Sun D, Wielinga P, Du G, et al. Mrp4 confers resistance to topotecan and protects the brain from chemotherapy. Mol Cell Biol 2004 ; 24 : 7612-21.
25) Lee YJ, Kusuhara H, Jonker JW, Schinkel AH, Sugiyama Y. Investigation of efflux transport of dehydroepiandrosterone sulfate and mitoxantrone at the mouse blood-brain barrier : a minor role of breast cancer resistance protein. J Pharmacol Exp Ther. (In press)
26) Kobayashi D, Ieiri I, Hirota T, Takane H, Maegawa S, Kigawa J, et al. Functional Assessment of Abcg2 (Bcrp) Gene Polymoephisms to Protein Expression in Human Placenta. Drug Metab Dispos. (In press)
27) Sparreboom A, Gelderblom H, Marsh S, Ahluwalia R, Obach R, Principe P, et al. Diflomotecan pharmacokinetics in relation to ABCG2 421C>A genotype. Clin Pharmacol Ther 2004 ; 76 : 38-44.

* * *

0013-7227/04/$15.00/0
Printed in U.S.A.

Endocrinology 145(9):4384–4391
Copyright © 2004 by The Endocrine Society
doi: 10.1210/en.2004-0058

Involvement of Multispecific Organic Anion Transporter, Oatp14 (*Slc21a14*), in the Transport of Thyroxine across the Blood-Brain Barrier

KIMIO TOHYAMA, HIROYUKI KUSUHARA, AND YUICHI SUGIYAMA

Department of Molecular Pharmacokinetics, Graduate School of Pharmaceutical Sciences, University of Tokyo, Tokyo 113-0033, Japan

The present study was aimed at investigating the involvement of mouse organic anion transporting polypeptide 14 (mOatp14) in the uptake of T_4 across the blood-brain barrier. Functional expression of mOatp14 in HEK293 cells revealed that T_4 and rT_3 are high affinity substrates of mOatp14 (Michaelis constant, 0.34 and 0.46 μM, respectively), and the specific uptake of T_3 was 4-fold less than that of T_4 and rT_3. Taurocholate, probenecid, and estrone-3-sulfate were moderate inhibitors for mOatp14, whereas digoxin (substrate of Oatp2), benzylpenicillin (substrate of Oat3), and large neutral amino acids had no effect. mOatp14 is widely expressed throughout the brain, except for the cerebellum. The expression of mOatp14 in the isolated brain capillaries and the choroid plexus was shown by Western blot. The uptake clearance of T_4 by the cerebral cortex determined using the *in situ* brain perfusion technique in mice was 580 μl/min·g tissue, 3-fold greater than that by the cerebellum, and a saturable component (Michaelis constant, 1.0 μM) accounts for the major fraction of the total uptake. Taurocholate inhibited the uptake of T_4 by the cerebral cortex completely, but the inhibition by estrone-3-sulfate was partial (50%). These results suggest that transporters play a predominant role in the delivery of T_4 to the brain, and mOatp14 accounts for estrone-3-sulfate inhibitable fraction, at least partly. The absence of inhibition by digoxin, benzylpenicillin, leucine, and 2-aminobicyclo-(2,2,1)-heptane-2-carboxylic acid for the uptake of T_4 by the cerebral cortex suggests the presence of other unknown transporter for T_4 uptake by the brain. Immunohistochemical staining revealed basolateral localization of mOatp14 in the choroid plexus in which it may also play a role in T_4 uptake. (*Endocrinology* 145: 4384–4391, 2004)

THYROID HORMONE IS critically involved in development and function of the central nervous system. Severe hypothyroidism during the neonatal period leads to structural alterations, including hypomyelination and defects in cell migration and differentiation, with long-lasting and irreversible effects on behavior and performance, whereas severe hyperthyroidism leads to a series of clinical manifestations, including neurologic and psychiatric symptoms (1). In adults, a number of neurological and psychological symptoms, which can be corrected by proper adjustment of the circulatory thyroid hormones, develops depending on the alterations in thyroid state (2).

The thyroid hormones are produced by the thyroid gland. L-T4, the prehormone, is the major form in the circulating blood and is converted to the active form, T_3, by the iodothyronine-deiodinase in peripheral organs. T_3 exerts its action through the nuclear receptors and regulates the expression of genes, such as nerve growth factor, tropomyosin-related kinase A (trkA), and common neutrotrophin receptor p75 ($p75^{NTR}$), in the brain (3). It has been proposed that serum-free T_4 and T_3 concentrations correlate with the activity level of thyroid hormone-dependent processes (free hormone hypothesis) (4). To exert their effect in the central nervous system, free thyroid hormones in the circulating blood have to cross the barriers of central nervous systems, the blood-brain (BBB) and the blood-cerebrospinal fluid barriers formed by the brain capillary endothelial cells and choroid plexus epithelial cells, respectively. Dratman and colleagues (5, 6) investigated the contribution of the transport via these pathways to thyroid hormone delivery to the central nervous system using autoradiography. The distribution of radioactivity associated with T_4, T_3, and rT_3 was limited to the circumventricular organs after intracerebroventricular administration, and so the transport across the BBB is considered to be a major pathway for the delivery of thyroid hormones in the circulating blood to regions of the brain (5, 6).

BBB is formed by brain capillary endothelial cells, which are characterized by highly developed tight junctions and a paucity of fenestra and pinocytotic vesicles. Due to these characteristics, they act as a physical barrier to separate the brain extracellular fluid from the circulating blood. Pardridge (7) demonstrated saturable uptake of T_3 by the brain using the intracarotid injection method (Brain Uptake Index method) and suggested that there is a specific transport mechanism for T_3 at the BBB. However, the transport mechanism for T_4 across the BBB remains controversial. The uptake of T_4 by the brain has been reported to be saturable in dogs (8) but nonsaturable in mice (9). The reason for this discrepancy remains unknown.

Abbreviations: BBB, Blood-brain barrier; BCH, 2-aminobicyclo-(2,2,1)-heptane-2-carboxylic acid; dpm, decay per minute; $E_2$17βG, 17β-estradiol-D-17β-glucuronide; E-sul, estrone-3-sulfate; K_i, inhibition constant; K_m, Michaelis-Menten constant; Leu, leucine; MCT8, monocarboxylate transporter 8; mOatp14, mouse Oatp14; Oatp14, organic anion transporting polypeptide 14; rOatp14, rat Oatp14; V_{brain}, volume of brain distribution; V_{max}, maximum uptake rate.

Endocrinology is published monthly by The Endocrine Society (http://www.endo-society.org), the foremost professional society serving the endocrine community.